Mapping the Ocean Current Strength and Persistence in the Agulhas to Inform Marine Energy Development

I. Meyer, L. Braby, M. Krug and B. Backeberg

Introduction

Renewable energy technology has undergone tremendous development over the last three decades and has found great commercial success in the onshore and offshore wind, solar, and biomass spheres. Of the renewable energy technologies, ocean energy technology is the least developed, and due to the vastness of the resource, many facets are yet to be fully understood. Energy in the world's oceans is found in either kinetic (i.e. waves, tides, or currents) or potential (i.e. thermal or salinity gradients) forms, and all forms are being investigated to generate useful electric power.

I. Meyer (✉)
Centre for Renewable and Sustainable Energy Studies,
Stellenbosch University, Stellenbosch, South Africa
e-mail: imke.meyer90@gmail.com; imke@sun.ac.za

M. Krug
Earth Observations, Natural Resources and the Environment,
CSIR, Stellenbosch, South Africa
e-mail: mkrug@csir.co.za

B. Backeberg
Coastal Systems, Natural Resources and the Environment,
Council for Scientific and Industrial Research, Stellenbosch, South Africa
e-mail: bbackeberg@csir.co.za

L. Braby · M. Krug · B. Backeberg
Nansen-Tutu Centre for Marine Environmental Research,
Department of Oceanography, University of Cape Town,
Cape Town, South Africa
e-mail: laurabraby@gmail.com

B. Backeberg
Nansen Environmental and Remote Sensing Center, Bergen, Norway

Z. Yang and A. Copping (eds.), *Marine Renewable Energy*,
DOI 10.1007/978-3-319-53536-4_8

The focus of this study is ocean current energy, the kinetic energy available in large-scale open-ocean geostrophic surface currents, and specifically the Agulhas Current. Western boundary ocean currents have become an area of focus (Duerr and Dhanak 2012; Chang et al. 2015), and the Agulhas Current is of specific interest in the Southern Hemisphere (Meyer et al. 2014; VanZwieten et al. 2014, 2015). Each ocean current has its own features but most western boundary currents have similar characteristics. Western boundary currents are narrow, intense, flow poleward, and are driven by the zonally integrated wind stress curl of the adjacent basins (Lutjeharms 2006).

Western boundary currents generally exhibit their strongest flow near the ocean's surface. In recent years, interest in these currents has evolved closer to commercial development, so the physical characteristics of the currents and their possible impacts on power generation need to be identified and fully understood. Ocean current resource characterisation studies have been performed for the Gulf Stream in the United States (Duerr and Dhanak 2012; Haas et al. 2013) and the Kuroshio Current near Japan and Taiwan (Chen 2010). Studies of the Agulhas Current on the East Coast of South Africa (e.g. Lutjeharms 2006; Beal and Bryden 1999; Bryden et al. 2005) have focused predominantly on understanding open-ocean oceanographic and climate-related processes. Few studies focus on characterising the Agulhas Current for ocean energy extraction technologies; in particular, the ocean current dynamics near the continental shelf region where technology deployment is possible are poorly understood.

Western boundary currents have the potential to be more reliable sources of energy than erratic winds because of their inherent reliability, persistence, and strength. Further, water is approximately 1,000 times denser than air resulting in high energy density in the oceans. Recent investigations by Haas et al. (2013) have shown that the Gulf Stream could potentially have an average power dissipation of 18.6 GW or 163 TWh/yr (serving the electricity needs of approximately 16 million households). According to the Ocean Energy Council, "Ocean currents are one of the largest untapped renewable energy resource on the planet. Preliminary surveys show a global potential of over 450,000 MW, representing a market of more than US$550 billion" (Renewable Energy Caribbean 2014).

The Agulhas Current flows southward along South Africa's East Coast, as a fast and narrow stream, and transports on average 70 million cubic metres of water per second (Bryden et al. 2005). Studies of the northern extent (north of 35ºS) of the current have shown that its course closely follows the narrow continental shelf (Gründlingh 1983), meandering less than 15 km from its mean path, and that the core of the current lies within 31 km from the coast almost 80% of the time (Bryden et al. 2005). The intensity of the current, its close proximity to the coast, and its relative stability make the Agulhas Current one of the more attractive ocean currents in the world to exploit for energy extraction.

However, the stable trajectory of the current is intermittently interrupted by perturbations known as Natal Pulses—large solitary meanders that form at the Natal Bight, a region between 29 and 30°S, and propagate downstream in the Agulhas Current at ±10 km/day (Lutjeharms and Roberts 1988). Fluctuations in the Agulhas

Current path associated with these meanders do not display the same frequency characteristics at all latitudes (Rouault and Penven 2011), because of the dissipation mechanisms of the Natal Pulses as they propagate downstream. Variability in the current and its velocities occurs across of a range of temporal and spatial scales (Lutjeharms 2006), and understanding, monitoring, and predicting these are vital for the effective use of the Agulhas Current as a renewable energy resource.

One of the most effective ways to monitor ocean currents over large spatial areas at a relatively high temporal frequency is through the use of satellite measurements. While ocean currents cannot be directly measured from space at present (Dohan and Maximenko 2010), surface current information can be derived from a range of remotely sensed observations to study and monitor the ocean circulation. At the larger scales (tens of kilometres), geostrophic currents, which occur as a result of pressure and Coriolis forcing, often drive most of the circulation. Wind stress at the ocean's surface also drives transport that can be estimated using the Ekman theory (Ekman 1905). Satellite observations of ocean surface winds and sea surface height (SSH) have therefore widely been used over the last two decades to study and monitor ocean circulation (Robinson 2004). Other remote-sensing observations such as Sea Surface Temperature (SST) and sea surface roughness can also be used routinely and systematically to derive ocean current information. The Agulhas Current is associated with strong signatures in SSH, SST, and sea surface roughness, all of which have been exploited successfully to study the variability of the Agulhas Current as demonstrated by Rouault et al. (2010), Rouault and Penven (2011), and Krug and Tournadre (2012). When used in synergy with the global network of in situ surface drifters, satellites can provide improved global observations of the sea surface velocity.

However, satellite measurements are limited to the surface and for the purpose of marine energy extraction, it is important to have information about the vertical structure of the water column. Measurements of the vertical structure of the ocean are even sparser. To deal with the spatially and temporally incoherent observations of the oceans, we use numerical models combined with observations through a process called data assimilation. Realistic simulations of the Agulhas system are complicated by the highly nonlinear nature of the mesoscale variability governing the Agulhas Current (Biastoch et al. 2008). Even if a model is capable of representing the mean circulation and variability of the region, inaccuracies in the initial state estimate inhibit the forecast skill of the model up to the decadal time scale (Meehl et al. 2009). Data assimilation provides the means to estimate a physically consistent three-dimensional (3D) estimate of the ocean state, combining a dynamical forecast model and observations together with their relative errors. Due to inaccurate numerics and boundary conditions, model solutions are imperfect. By repeatedly assimilating data, models may be constrained to provide a more realistic estimate of the ocean state. Such data-assimilative models of the ocean play a vital role in predicting ocean currents as well as in understanding the 3D structure and its variability.

By combining state-of-the-art satellite remote-sensing observations with data-assimilative (predictive) ocean models, this study aims to identify areas of energetic flow along South Africa's East Coast for the purpose of marine energy

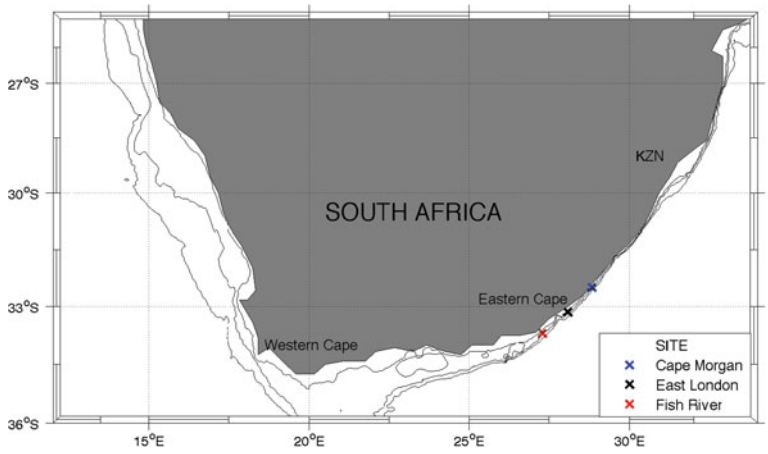

Fig. 1 Position of ADCP deployments with 100, 200, and 500 m isobaths

extraction and to examine the associated current characteristics. The ability and usefulness of the satellite remote-sensing observations and predictive models to monitor and predict current velocities and their variability will be assessed by comparing them with in situ velocity measurements from Acoustic Doppler Current Profilers (ADCPs) for the period from 2009 to 2010. In doing so, the impact of the current behaviour on the potential power production will be quantified, and the present day state-of-the-art tools used to accurately monitor and predict fluctuations in the Agulhas Current that affect power production will be critically examined.

The focus area for the analysis lies between the latitudes of 31 and 34°S as indicated in Fig. 1. The coastal proximity and strength of the Agulhas Current in the southeast Agulhas Current region make it the most suitable region for energy exploitation. Farther south, the Agulhas Current flows too far from the coast to allow for efficient energy recovery. Farther north, the current strength is decreased.

This chapter examines the Agulhas Current characteristics and attempts to quantify how its behaviour will affect potential power production. In the following section, the available data and data types are described, followed by an investigation of current strength and variability, the usefulness of the various data sets, and the implications for possible energy production. The technical, environmental, and social impacts of harnessing energy from the Agulhas Current are also considered.

Data and Methods

The data sets described in the following sections are used to determine the physical characteristics of the Agulhas Current. The sections also address the relative usefulness of each data set towards reducing the barriers of entry into the ocean current energy market.

GlobCurrent Data Set

In this study, we use the combined 15-m-depth GlobCurrent Version 2 product, which is available from the GlobCurrent project (http://www.globcurrent.org/). This data set consists of 13 years of global gridded ocean current fields and is provided at a 0.12° spatial resolution and 3-hour time interval. The combined current in the GlobCurrent data set is computed as the sum of the geostrophic and Ekman components of the flow. In the GlobCurrent product, geostrophic currents are derived from satellite observations of SSH from multiple altimeters, while the Ekman currents (driven by local wind forcing) are estimated using Lagrangian ocean current information collected from surface drifters and Argo floats. A detailed description of the method used to derive the GlobCurrent geostrophic and Ekman ocean currents is provided by Rio et al. (2014).

Confirming the validity of using satellite data to monitor the behaviour of the Agulhas Current is crucial to reducing the costs of monitoring the operations of a potential ocean current plant as well as monitoring upstream events that can affect the potential power output of a plant.

Global Hybrid Coordinate Ocean Model

3D ocean forecast data from a global Hybrid Coordinate Ocean Model (HYCOM) are used in this study. These data are freely available from the HYCOM consortium (hycom.org), a multi-institutional effort sponsored by the National Ocean Partnership Program, as part of the U.S. Global Ocean Data Assimilation Experiment, to develop and evaluate a data-assimilative hybrid isopycnal-sigma-pressure (generalised) coordinate ocean model.

The numerical model is configured for the global ocean, and computations are carried out on a Mercator grid between 78°S and 47°N at 1/12° (± 7 km) resolution. There are 32 vertical layers, and the model's bathymetry is derived from a quality-controlled Naval Research Laboratory Digital Bathymetry Data Base 2-minute resolution data set. Surface forcing data are from the Navy Operational Global Atmospheric Prediction System and include wind stress, wind speed, heat flux (using bulk formula), and precipitation.

The data assimilation scheme used is the Navy Coupled Ocean Data Assimilation system (Cummings 2005), which uses the model forecast as a first guess in a Multi-Variate Optimal Interpolation scheme and assimilates available along-track satellite altimeter observations (obtained via the NAVOCEANO Altimeter Data Fusion Center), satellite and in situ SST as well as available in situ vertical temperature and salinity profiles from Expendable BathyThermographs, ARGO floats, and moored buoys. The surface measurements are projected to the model interior using the Modular Ocean Data Assimilation System (Fox et al. 2002).

On a daily basis, 5-day hindcasts and 5-day forecasts are produced. The raw data are interpolated to 33 fixed horizontal levels, which are 0, 10, 20, 30, 50, 75, 100, 125, 150, 200, 250, 300, 400, 500, 600, 700, 800, 900, 1,000, 1,100, 1,200, 1,300, 1,400, 1,500, 1,750, 2,000, 2,500, 3,000, 3,500, 4,000, 4,500, 5,000, and 5,500 m.

U- and v-component velocities from 1 December, 2009 to 31 January, 2013 were downloaded and subset to 25–35ºE and 27–36ºS. The data were generated by two experiments. The first experiment (expt_90.8) ended on 2 January, 2011, after which expt_90.9 was used. The two experiments are subtly different in that the top layer in expt_90.9 was 1 m thick (as opposed to 3 m in expt_90.8). This difference is not expected to affect our analysis.

The ability to predict the behaviour of the Agulhas Current will be advantageous for the integration of any future power plants into the national power pool. Accurate forecasts at a high temporal resolution will ensure the maximum utilisation of an ocean current power plant.

Acoustic Doppler Current Profilers

Between 2005 and 2010, the South African electricity utility, Eskom, conducted a series of in situ current measurements along the eastern shores of South Africa as part of a preliminary assessment of the Agulhas Current as a source of energy. The in situ ocean currents were measured using moored ADCPs at selected sites along the continental shelf and in water depths ranging from 96 to 60 m. All ADCPs sampled ocean current velocities throughout the water column in 2-m-high vertical bins. Bins from different deployments were concatenated by linking together measurements from the closest bin (nearest bin approach). A summary of this ADCP data is provided in Table 1.

It is observed that the ADCP measurements (Table 1) were taken at the periphery of the current. Rouault and Penven (2011) found that near the location of the East London, the landward edge of the Agulhas Current is generally lies 20 km from the shore and above the 100 m isobath. Note that the dates on which each data set was recorded do not coincide and this can possibly lead to a bias towards one site.

Between 2012 and mid-2013, an additional two ADCPs were deployed at a mid-shelf and offshore location and resulted in an 18-month period of continuous data in the region of 28.8°E and 32.5°S. The details of the captured data are outlined in Table 2. The data were collected using Teledyne RDI ADCPs with a 60-min temporal resolution. Viable data for the mid-shelf location range from 84 to 10 m below the sea surface and for the offshore location, and from 238 to 22 m below the sea surface.

Table 1 Details of in situ ADCP measurements

ADCP site name	Instrument type	Longitude (E)	Latitude (S)	Water depth (m)	Record length	Sampling interval (h)
Cape Morgan CM305	RDI 300	28.83183	32.50733	89	2009/12/05-2010/03/03	1
Cape Morgan CM306	RDI 300	28.83179	32.50725	87	2010/03/03-2010/09/13	1
Fish River FR308	RDI 300	27.29750	33.70335	88	2009/12/04-2010/03/04	1
Fish River FR309	RDI 300	27.29745	33.71332	91	2010/03/04-2010/09/03	1
East London EL314	RDI 300	28.00866	32.15145	82	2009/12/04-2010/03/03	1
East London EL315	RDI 300	28.08651	33.15140	85	2010/03/03-2010/09/13	1

Table 2 Deployment series 2: details of available ADCP data

Location	ADCP type/bin resolution (m)	Distance from shore (km)	Time period	Sounding depth (m)
Mid-shelf	RDI 300/2	14	2012/01/24-2013/06/30	91
Offshore (edge of shelf)	RDI 150/6	18	2012/01/24-2013/06/30	255

Current Strength and Variability

Comparison GlobCurrent, HYCOM, ADCPs

To compare the three ocean velocity products, Principal Component Analysis (PCA) was applied to the ADCP velocity data as well as the GlobCurrent and HYCOM data at the same locations (Cape Morgan, East London, and Fish River) and depths. PCA decomposes data in terms of orthogonal basis functions to find time series and spatial patterns (Wold et al. 1987). The two eigenvectors contain most of the details about the data. They were computed and plotted as 95% confidence interval ellipses in Fig. 2 and represent the two dominant directional modes of the measured current velocities at the three selected locations, indicating the dominant current direction as well as its lateral variation.

Figure 2 provides a good overview of the Agulhas Current time-averaged strength as well as its overall variability. Comparisons between the in situ satellite and numerical model output data sets show distinct differences. From the in situ

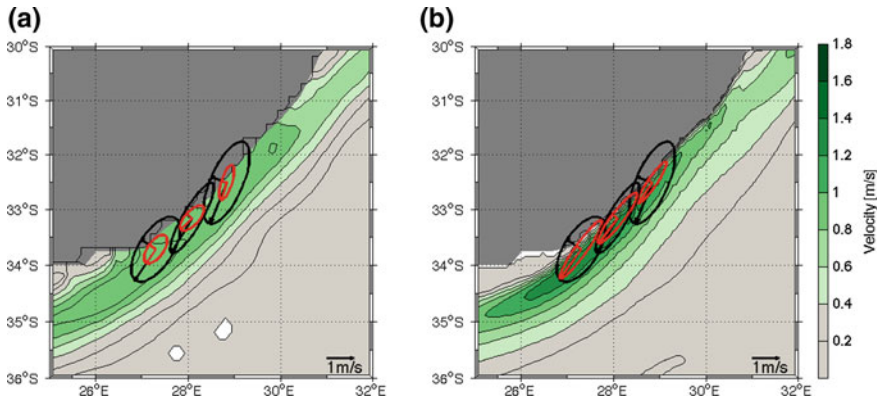

Fig. 2 **a** Map of Agulhas time-averaged currents from the GlobCurrent product with overlaid current ellipses from ADCP data (*black*, at 20 m or in the upper layer best suited for energy production) and GlobCurrent data (*red*, at 15 m depth), and **b** map of Agulhas time-averaged currents from the HYCOM product with overlaid current ellipses from ADCP data (*black*, at 20 m or in the upper layer best suited for energy production) and HYCOM data (*red*, at same depth as ADCPs)

ADCP data, it is seen that the Cape Morgan location is the most energetic and has the strongest major velocity component. This finding is reiterated by the GlobCurrent data but not by the HYCOM data.

Comparing the ADCP and GlobCurrent ellipses (Fig. 2a, black and red, respectively), it is evident that although the direction of flow is similar, there are significant differences between the two data sets at all three locations. The ADCP data indicate a much stronger south-westward flowing velocity component with larger lateral variations compared to the GlobCurrent data.

The HYCOM velocity map (Fig. 2b) indicates that the data-assimilative modelling system is able to produce high mean velocities, and comparing the HYCOM ellipses to the ADCP ellipses suggests that the mean south-westward component is better represented than in GlobCurrent, but the lateral variability seems to be reduced in HYCOM.

In agreement with the current ellipses (Fig. 2a), the major and minor velocity components summarised in Table 3 confirm that the GlobCurrent data underestimate the ADCP measured current velocity by ±60%. While there is a slight improvement in HYCOM, the data-assimilative modelling system still underestimates the measured ADCP velocities (Table 4). It is important to note the differences between satellites remotely sensed, modelled, and in situ observed data because these differences could lead to incorrect site selection and evaluations for energy production. Further, if the HYCOM data set is used as a first step towards identifying energetic regions prior to deploying in situ measurement devices, this data set would lead to incorrect assumptions about the most energetic region. Further, the significant under prediction seen in the GlobCurrent data set can result in termination of further exploration.

Table 3 Details of the time-averaged velocity vector lengths of the GlobCurrent and ADCP measurements

Site name	ADCP data		GlobCurrent	
	Major component (m/s)	Minor component (m/s)	Major component (m/s)	Minor component (m/s)
CM	1.6710	0.6850	0.6815	0.2377
EL	1.5496	0.3959	0.6475	0.2769
FR	1.4216	0.6997	0.6564	0.3251

Table 4 Details of the time-averaged velocity vector lengths of the HYCOM and ADCP measurements

Site name	ADCP data		HYCOM	
	Major component (m/s)	Minor component (m/s)	Major component (m/s)	Minor component (m/s)
CM	1.6710	0.6850	0.9794	0.1918
EL	1.5496	0.3959	1.2333	0.2542
FR	1.4216	0.6997	1.3730	0.2443

The observed underestimation of both GlobCurrent and HYCOM may have to do with the temporal averaging of the data in their generation. The regularly gridded satellite data (GlobCurrent) are produced using optimal interpolation and merging techniques to fill the gaps between spatially sparse satellite ground tracks. This merging process results in the smoothing of the data in both space and time (Ducet et al. 2000) and the underestimation of the ocean current velocities. The underestimation observed in HYCOM may be associated with the combined effect of the model itself underestimating the currents in addition to the assimilation of satellite products into the model.

The impact of spatial and temporal smoothing is examined below, by performing a spectral analysis (Fig. 3), whereby the dominant frequencies of variability in the three data sets are compared. Then, temporal smoothing (daily, weekly, 10-daily, and monthly) is applied to the ADCP data and plotted in a Taylor Diagram (Fig. 4), which is a way to graphically summarise how closely a set of data matches a reference data set (in this case the hourly ADCP data).

A spectral analysis essentially transforms magnitude—time data into variance—frequency space. Figure 3 shows the spectra from the ADCP data (a), GlobCurrent data (b), and HYCOM data (c) for the Cape Morgan and East London locations.

Variability in the Agulhas Current can occur at a number of time scales, which is evident from examining the ADCP data. Some examples of variability include tides, sub-mesoscale and mesoscale eddies, Natal Pulses, seasonal variations in current velocities (Krug and Tournadre 2012), and longer term variations associated with climate modes such as the El Niño Southern Oscillation and gyre circulation changes. The ADCP spectra were compared with the GlobCurrent and HYCOM

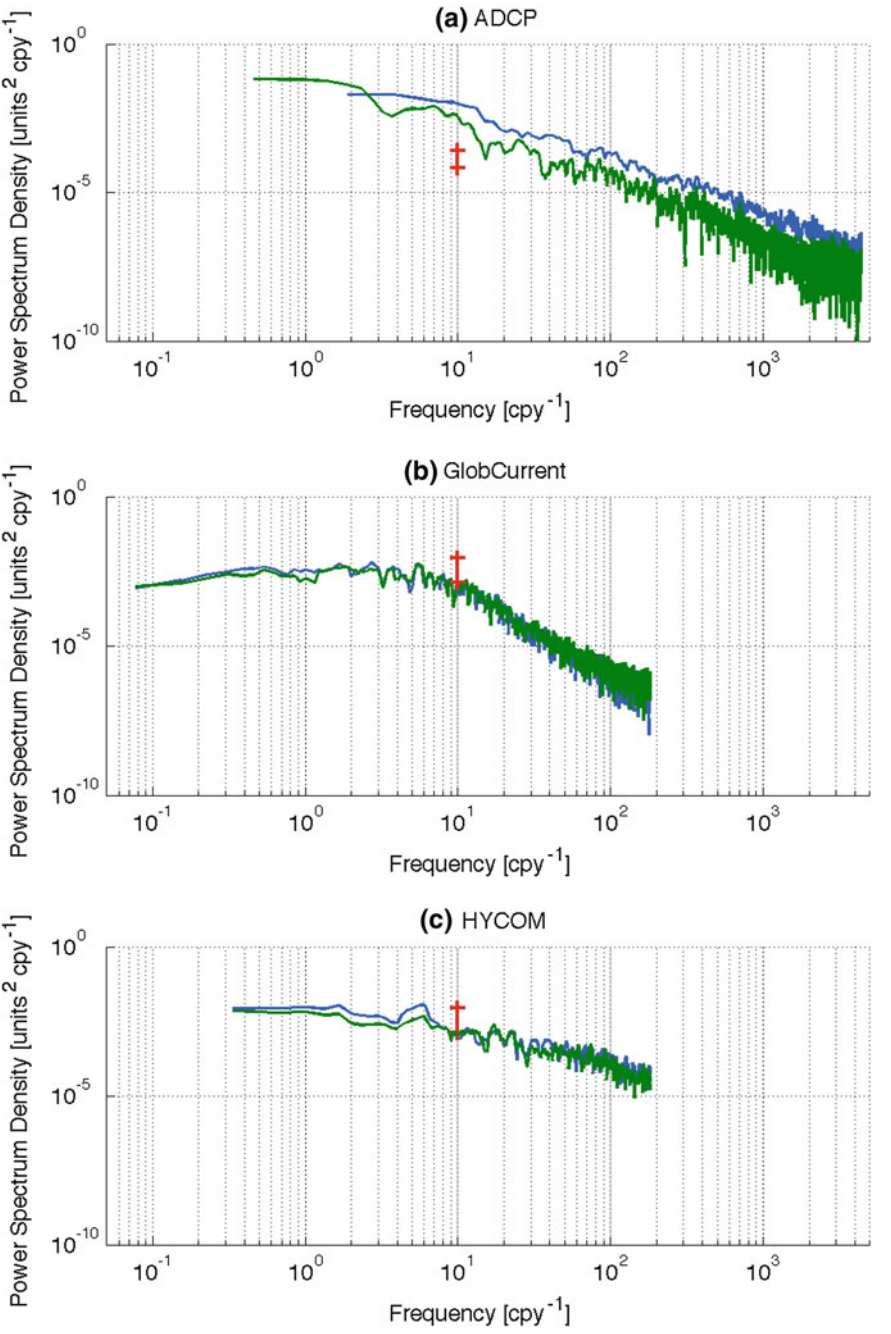

Fig. 3 Spectra at selected sites—Cape Morgan (*green*) and East London (*blue*)—using **a** ADCP data for record data lengths of 193 days (*green*) and 137 days (*blue*), **b** GlobCurrent data for a record data length of 14 years, and **c** HYCOM data for a record data length of 3 years. The *red* line indicates the 95% significance level

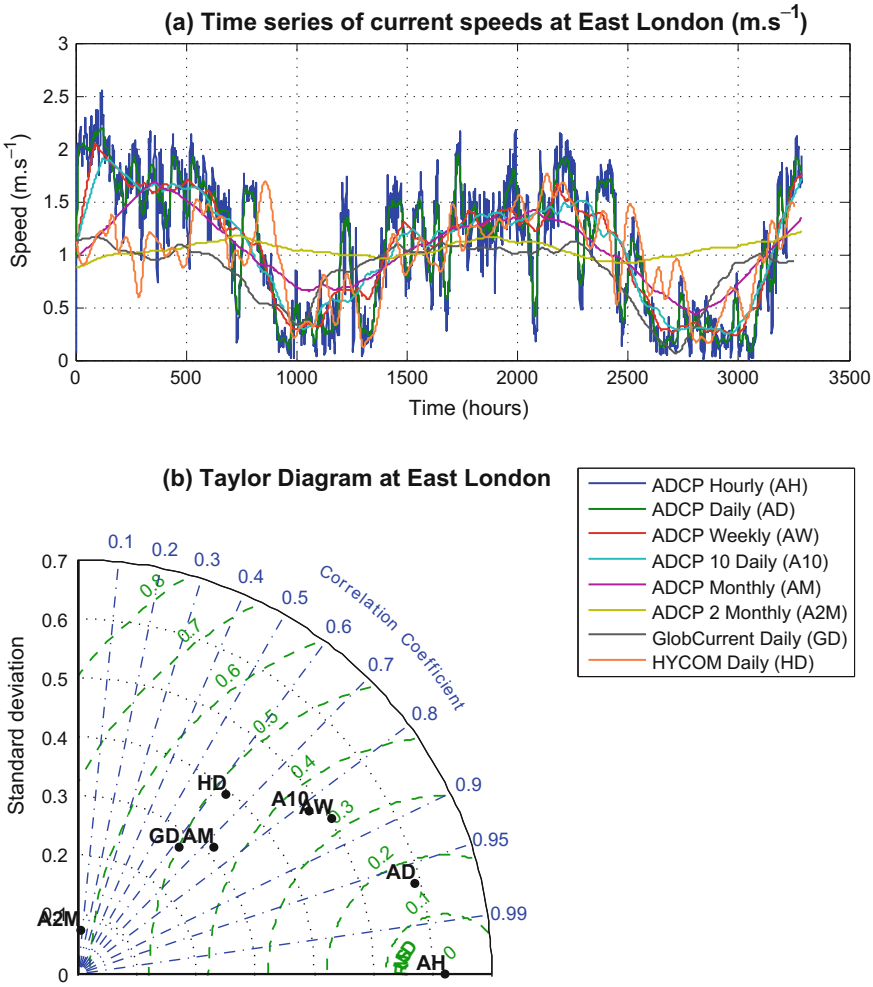

Fig. 4 **a** A time series of Agulhas Current speeds (m/s) at East London using hourly, daily, weekly, 10-daily, monthly, and 2-monthly ADCP data as well as daily GlobCurrent and HYCOM data at the same location. **b** A Taylor Diagram showing the standard deviation, correlation, and centred root-mean-square difference of the same data sets at East London

spectra to evaluate the accuracy of the modelled and satellite-derived velocities with respect to these modes of variability.

Comparing the three data sets, it is evident that there is very little difference between the Cape Morgan and East London spectra in the GlobCurrent and HYCOM data sets. The ADCP data set, however, shows a higher spectrum density at the East London location. This suggests that there are slightly higher levels of variability at East London compared to Cape Morgan, which is in agreement with the PCA analysis (Fig. 2).

To determine the frequency of the dominant mode of variability, one evaluates where the strongest change in the slope of the spectra occurs. The x-axis of Fig. 3 represents frequency, where 100 is 1 cycle per year. Each successive vertical grid line to the right is one additional cycle per year. Thus, the GlobCurrent data indicate a predominant mode of variability of six cycles per year (two-monthly), which may be related to the passage of Natal Pulses or other Agulhas Current meanders. This two-monthly cycle is also present in HYCOM, but the change in slope is much weaker, and therefore, the signal is not significant. The lengths of the ADCP time series (193 days at Cape Morgan, 137 days at East London,) are too short to confidently confirm the two-monthly dominant mode of variability.

Typically, spectra of ocean processes should have steep slopes, which signify an inverse cascade of energy from low frequencies to high frequencies (e.g. hourly to monthly) (Scott and Wang 2005). The slopes in the spectra of the ADCP and GlobCurrent data sets are in good agreement with each other, indicating a rapid decay in the ocean current energy towards high frequency. At higher frequencies (101–102), the HYCOM data set has more energy compared to the ADCP and GlobCurrent data sets, but the slope is flatter indicating that all frequencies have similar levels of energy, which is indicative of white noise. The flatter slope in the HYCOM data set shows that energy decay in the model is inadequately simulated and that in the assimilated model output, there are no coherent processes producing an inverse energy cascade. The fact that the slopes of the inverse energy cascade in the spectra of GlobCurrent and the ADCP data agree indicates that both data sets are able to capture the larger (meso) scale processes that dominate the energy spectra. Comparatively, the higher frequency variability is relatively less important, as is evident in the flattening of the slope.

Figure 4a shows the time series of the hourly ADCP data, the daily, weekly, 10-daily, monthly, and 2-monthly averaged ADCP data, as well as the GlobCurrent and HYCOM daily data for East London. The comparison highlights the impact of temporally averaged data as well as the variability captured by the temporally smoothed ADCP data and the daily satellite and modelled data products. The correlation coefficient, standard deviation, and root-mean-square difference (RMSD) of the temporally averaged ADCP data together with the GlobCurrent and HYCOM data are summarised in the Taylor Diagram (Fig. 4b).

As expected, the correlation coefficient and standard deviation decrease, concurrently with increasing RMSD when the ADCP is averaged over increasingly longer time periods (i.e. hourly to daily to weekly to monthly to two-monthly).

Using the hourly ADCP data as a reference, and comparing the respective daily, weekly, 10-daily, monthly, and 2-monthly averaged ADCP data to the daily GlobCurrent and HYCOM data, suggests that HYCOM and GlobCurrent are only able to accurately represent variability occurring at the monthly time scale. This is indicated by the fact that the monthly ADCP data and the GlobCurrent and HYCOM daily data are clustered around similar correlation coefficients, standard deviations, and RMSDs.

These results have significant implications for the ability to use state-of-the-art satellite remotely sensed and assimilative modelling products when determining

potential energy extraction sites. Furthermore, the ability to use these tools to predict variability in the Agulhas Current is questionable at this stage, and this highlights the need for further development and improvement of these products. Nevertheless, in the absence of a spatial and temporally coherent ocean observing system for the Agulhas Current, these data provide useful insights into the modes of variability of the Agulhas Current and their implications for energy production.

Implications for Energy Production

For resource measurements to be useful in monitoring or predicting behaviour, the temporal resolution of the data used in the prediction need to be able to capture the temporal variability associated with the ocean processes to be predicted. For example, if significant variability is seen at an hourly resolution, then the monitoring equipment needs to be able to accurately capture this variability to be able to successfully control a potential ocean current power plant. As noted in the above analysis, in situ ADCP data are the only data at present that can accurately capture the full variability of the Agulhas Current, but deploying and managing ADCP devices are costly and spatially limiting. In the absence of ADCP data, the only alternative data sources are those derived from satellite remote-sensing measurements and data-assimilative predictive models. In the previous section, it is shown that the correlation between data obtained from the ADCPs and those obtained from the Globcurrent and HYCOM products only compare well on a monthly scale and thus have limited use in assisting in monitoring and predicting the shorter time scales of variability in the Agulhas Current. Additionally, satellite remote-sensing observations are limited to the surface level, so it is important to note that there is a need for the characteristics throughout the depth of the water column to characterise to be useful in monitoring and predicating energy output from this resource.

Figure 5 shows time series ADCP data plots of velocity versus depth highlighting the variability of the Agulhas Current. The presence of major events of variability—a Natal Pulse—is recognised as a drop in the current speed to near zero throughout the water column for longer than 10 continuous days. This indicates that the current core has been displaced seaward from its original course by the Natal Pulse meander. All measurements taken at different latitudes have been plotted on the same temporal axis so that the propagation of a Natal Pulse southward along the coastline can be identified.

In Fig. 5a, the presence of four Natal Pulses, which occurred in Nov 09, Mar 10, May 10, and Aug 10 and each persisted for at least 20 days, is seen from November 2009 to September 2010. In Fig. 5c, it is seen that the Natal Pulses of November 2009–September 2010 in Fig. 5b did not dissipate as they travelled southward, and the presence of these pulses is seen in the data set in Fig. 5c.

Each of these pulses takes approximately 15–20 days to travel down the coast between the two locations. Similarly, the Natal Pulse that occurred in July 2008 travelled down the coast; the Pulse is first seen in the data set captured in Fig. 5a,

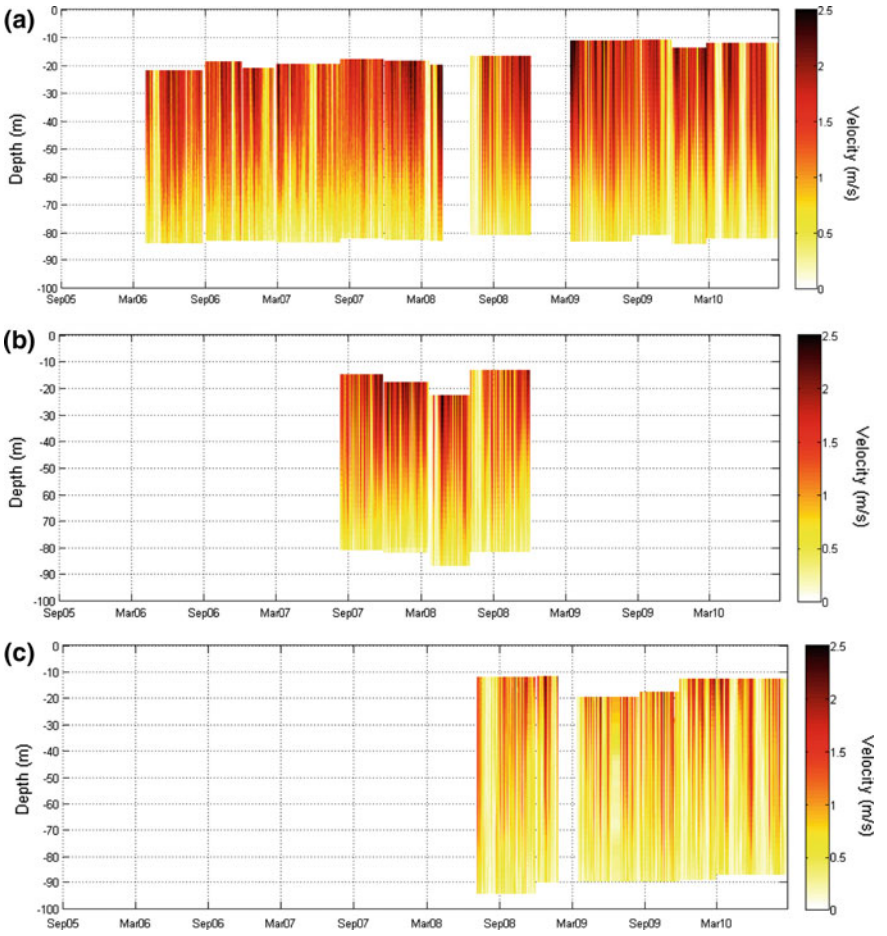

Fig. 5 Temporal plots of velocity magnitude versus depth at **a** Cape Morgan, **b** East London, and **c** Fish River

then again in the Fig. 5b data set, and lastly in the Fig. 5c data set. This Natal Pulse also takes approximately 15 days to arrive at the location plotted in Fig. 5c from the location plotted in Fig. 5a. The fact that the Natal Pulse took a fortnight to travel ~200 km is a testament to the sluggish velocity magnitude at which such pulses propagate.

Figure 5a, shows the results from two deployed ADCPs, one deployed from April 2006 to May 2008 and another from March 2009 to September 2010. When the two time periods are compared, the 24-month period from April 2006 to May 2008 only sees three pulses of approximately 10-days duration whereas during the 17-month period from March 2009 to September 2010 four Natal Pulses are observed. The difference in the occurrence of Natal Pulses at the same location over

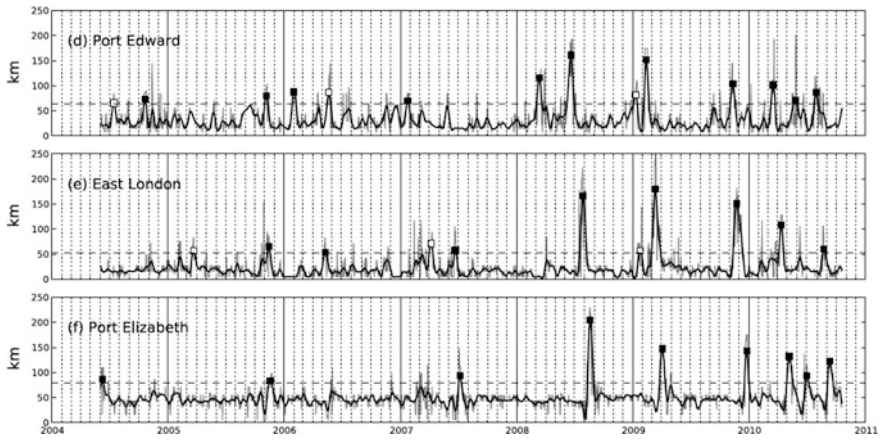

Fig. 6 Position of the Agulhas Current used to identify the presence of Natal Pulses. Natal Pulses are indicated by black squares, adapted from Fig. 5 in Rouault and Penven (2011)

different time periods shows the erratic and unpredictable nature of this phenomenon and emphasises the importance of anticipating such events.

The results found in the temporal velocity magnitude plots compare well with the results found by Rouault and Penven (2011). Figure 6 shows the position of the Agulhas Current inshore front relative to the shore at three locations along the coastline in order to determine the presence and propagation of Natal Pulses. It is promising to see the correlation between the in situ data presented in Fig. 5a and the satellite data used to plot Fig. 6e. From Fig. 6, it is seen that the occurrence of the four Natal Pulses from November 2009 to September 2010 is abnormally high; Rouault and Penven (2011) found the average to be 1.6 pulses a year when considering a 20-year period. Further, the same propagation trend down the coastline that was found in Fig. 5 is shown in Fig. 6.

The lag between the locations shows the sluggish nature of the phenomenon but can be used to the advantage of plant operators. If an ocean current power plant were to be installed in the energetic region of 32.5°S and the behaviour of the Agulhas Current were tracked further up the coast around 31.2°S, the presence of an approaching Natal Pulse could be predicted approximately two weeks in advance. Such tracking may be done using a remote-sensing technique, but the reduced correlation between in situ and satellite data at the weekly to 10-day time scale (Figs. 5 and 6) may hamper this ability.

A timely warning of the occurrence of Natal Pulses is critical, however, and will allow power grid operators to plan to use the period when a Natal Pulse is present for maintenance of the ocean current power plant. Furthermore, grid planners can mobilise other capacity to ensure the demand of the country is met. However, other available capacity may not be available during winter months when demand is high, and because there is no seasonal trend in the occurrence of Natal Pulses, there is risk related to the firm capacity of an ocean current power plant. The lengthy

presence of a pulse (~20 days) in one location is a concern for the technically possible capacity factor and the capability of ocean current energy to supply a reasonably uninterrupted supply of power to off-takers..

Characteristics of Energetic Region

From the analysis in current strength and variability section, of the data collected along the South African East Coast, the energetic region lies in the region of 28.8 E and 32.5 S (Cape Morgan location). This location has favourable velocities and because of the bathymetry in the region the current core lies in close proximity to the coast. The following analysis presents the physical characteristics of a mid-shelf and offshore site in this region.

Current Magnitude

Figure 7 shows the current velocity magnitude versus depth. A minimum, 75% exceedance, 50% exceedance, 15% exceedance, and the current maximum are plotted.

When comparing the two sites, the presence of the Agulhas core is seen clearly at the offshore location, where at water depths of 50 and 30 m the mean velocity magnitude is 1.49 and 1.59 m/s, respectively. For the mid-shelf deployment, the mean current velocity magnitude is 1.00 and 1.34 m/s at water depths of at 50 and 30 m, respectively. The mid-shelf mooring is thus placed at the core's edge. At the 30 m water depth, the offshore current velocity magnitude is 1.2 times greater than the mid-shelf velocity magnitude, which is when the cubed relationship between velocity magnitude and power is considered, results in a significant difference. The 75% exceedance values at the 30 m depth are 1.0 and 1.29 m/s for the mid-shelf and offshore deployments, respectively; the 75% exceedance values at the 50 m depth are 0.69 and 1.17 m/s for the respective deployments. A similar trend is seen for the 15% exceedance plot; values for the respective mid-shelf and offshore deployments at the 30 m depth are 1.91 and 2.16 m/s and at the 50 m depth they are 1.45 and 2.06 m/s. These ranges indicate that a turbine that is deployed in the Agulhas Current will need to operate at speeds between 0.6 and 2 m/s.

Figures 8 and 9 are temporal time series plots of time versus depth in which the colour scale indicates the current velocity magnitude for each location. These plots highlight the variability of the current velocity magnitude and show the erratic presence of day-long eddies and Natal Pulses. The distinct presence of a Natal Pulse is seen during April 2013, as indicated by the entire water column velocity magnitude dropping to near zero. The size of these meanders are realised because both sites are affected by this occurrence. Figures 8 and 9 show how problematic the presence of this phenomenon will be to potential power production from a turbine

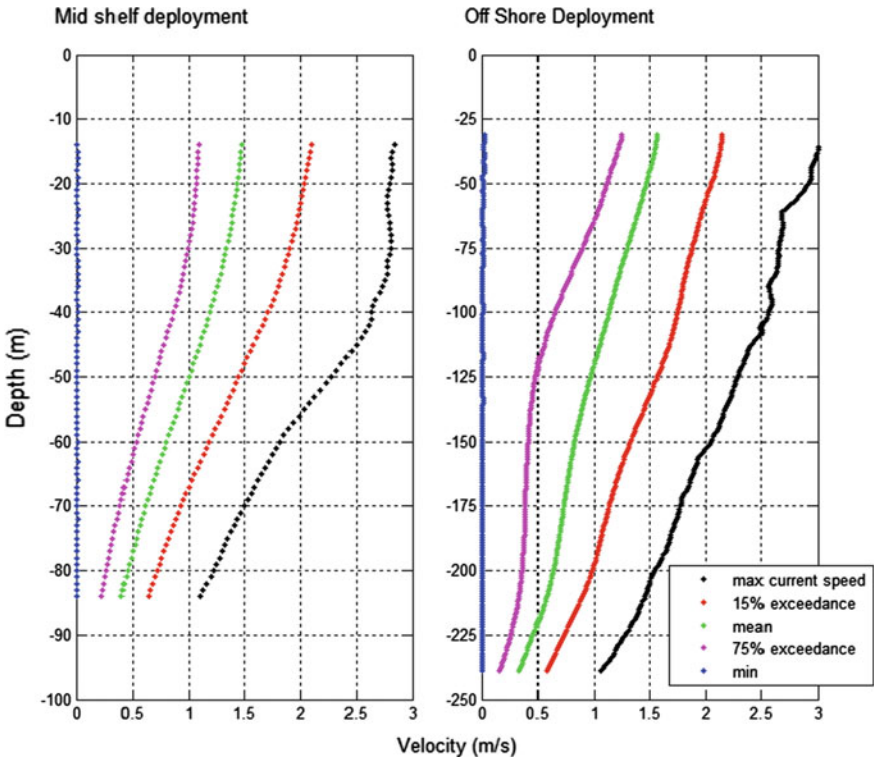

Fig. 7 Current velocity magnitude (m/s) ADCP minimum (*blue*), 75% (*magenta*), mean (*green*), 15% (*red*), and maximum (*black*) flow speeds at the mid-shelf (*left-hand* figure) and offshore (*right-hand* figure) locations (Meyer and Van Niekerk 2016)

array because all power production will stop during the presence of a Natal Pulse. Three other time periods of low velocity magnitude seen in these figures indicate the presence of eddies in the current core—during February 2012, May 2012, and October 2012. These eddies did not persist as long as the occurrence in April 2013, but such events add to the variability of the current and lower the availability of the current.

Rouault and Penven (2011) found an average of 1.6 Natal Pulses travel down the East Coast of South Africa annually. The data set evaluated here is 18 months long and has only one distinct occurrence present that can result in a more optimistic capacity factor for this period than in an average year. This shows that the measured in situ data sets cannot be used in isolation to quantify the performance of the current, but need to be compared to data sets that cover a longer period of time (10 years or more) to ensure correct trends are observed, and this can be achieved by using remote-sensing data.

Figures 10 and 11 show the velocity magnitude distribution and cumulative frequency of occurrence at the 30 and 50 m depths for each of the locations. In both

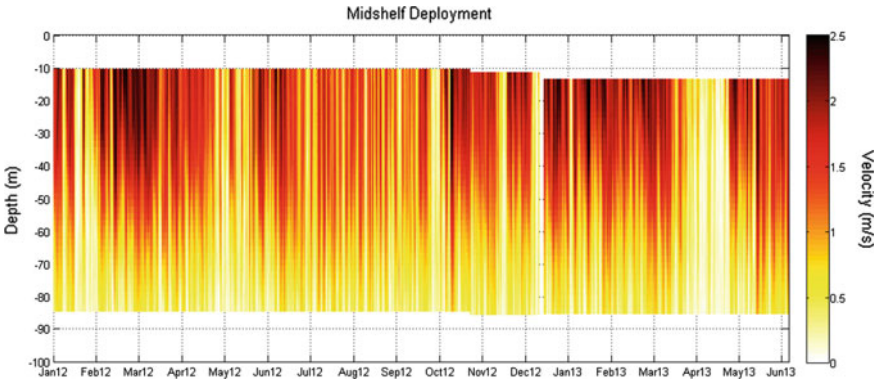

Fig. 8 Temporal plot at the mid-shelf location. Time versus depth with the colour scale indicating current speed (m/s) (Meyer and Van Niekerk 2016)

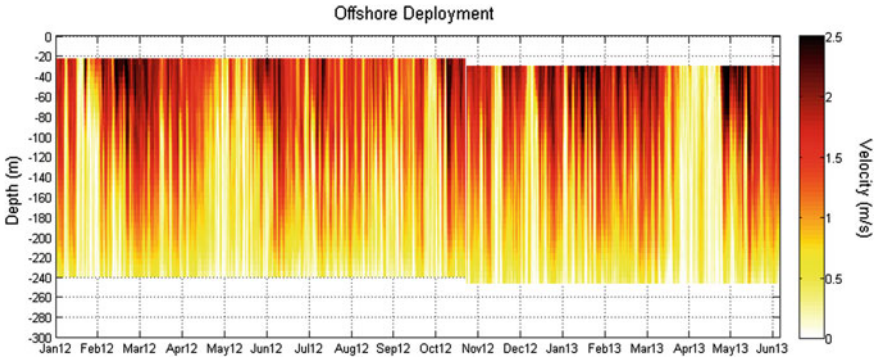

Fig. 9 Temporal plot at the offshore location. Time versus depth with the colour scale indicating current speed (m/s) (Meyer and Van Niekerk 2016)

Figs. 10 and 11, in the Frequency of Occurrence plot, two distinct peaks are seen: the first is low velocity magnitude peak, indicating the velocity magnitude distribution during the presence of a Natal Pulse or weekly eddies, and the second occurs when no such phenomena are present. The second peak tends to the bell shaped curve of a normal distribution curve, but is skewed to the left by low velocity magnitude values. This observed distribution must be noted when the mean velocity magnitude or mean power density is evaluated throughout the water column, because if the periods when Natal Pulses are present are treated as maintenance periods and are thus excluded, then the average velocity magnitude or power density will be higher than represented. However, as seen in Figs. 10 and 11, there are periods of low velocity magnitude that do not persist as long as Natal Pulses, but they will negatively affect potential power production and cannot be discounted.

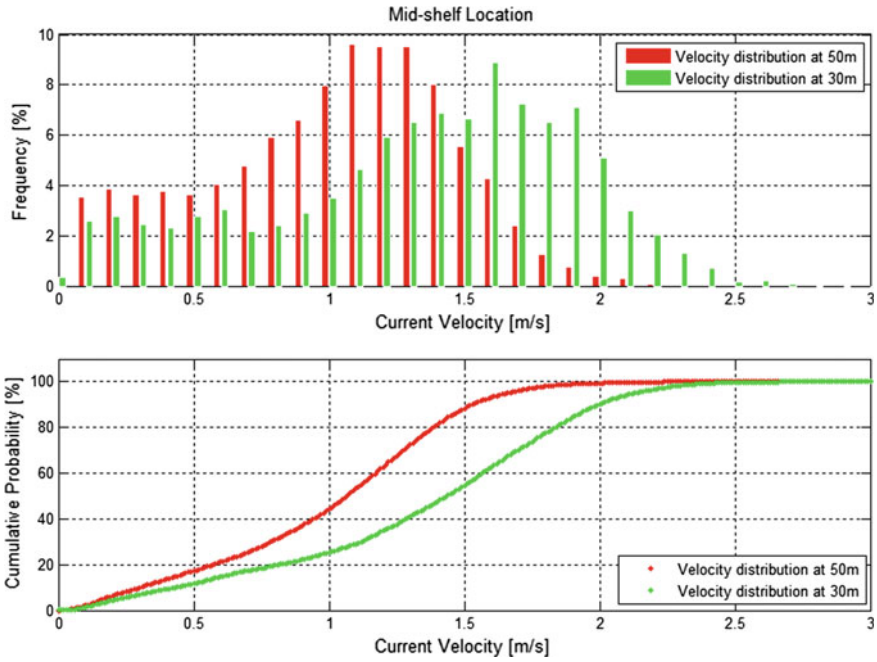

Fig. 10 Velocity magnitude distribution at the mid-shelf location (Meyer and Van Niekerk 2016)

The typical cut-in speed of marine turbines is between 0.5 and 1.0 m/s (Meyer and Van Niekerk 2016). If the velocity magnitude distribution is compared to these velocity magnitude values for both the mid-shelf and offshore location, one notes that the low velocity magnitude peak present in the full distribution curve will result in non-operational turbines.

In Figs. 10 and 11, the shift in the histogram bars towards the higher velocities for the shallower measurement highlights the difference in velocity magnitude seen at the 30 m depth compared to the 50 m depth. There is less of a difference between the velocities at the 30 and 50 m depths at the offshore location due to the deeper penetration of the current core at this site and lesser impact of seabed drag on the current. Furthermore, velocities at a 60 m water depth at the offshore location are comparable to the velocities at a 20 m depth at the mid-shelf location. This is important to note because deploying and mooring a turbine array at a sea bed depth of 255 m may prove to be challenging. Figure 8 through Fig. 11 reiterate the importance of mooring the turbine array as close to the surface as possible for maximum power output.

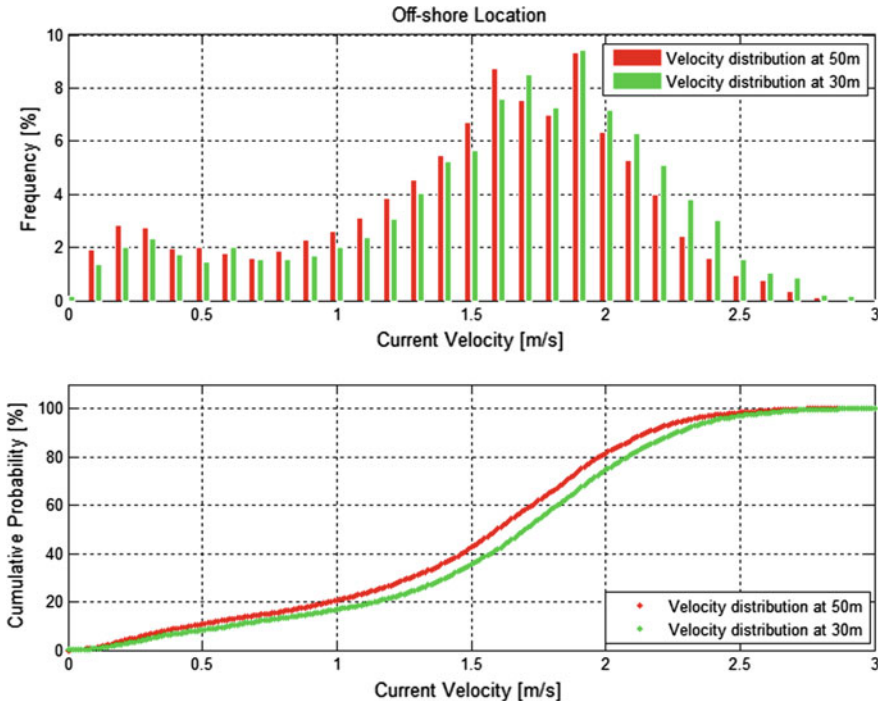

Fig. 11 Velocity magnitude distribution at the offshore location (Meyer and Van Niekerk 2016)

Power Density

The power density of a fluid stream across a unit cross section is given by:

$$P = \rho \frac{1}{2} v_{ins}^3 \tag{1}$$

where ρ is the density of the fluid and v_{ins} is the instantaneous velocity magnitude of the fluid stream.

The mean power density versus depth is plotted in Fig. 12. As noted in the velocity magnitude analysis, the power density at 20 m at the mid-shelf deployment (2,265 W/m^2) is similar to that at 60 m at the offshore deployment (2,180 W/m^2). At the 30 m water depth, the mean power density is 1,857 and 2,866 W/m^2 at the mid-shelf and offshore locations, respectively. The power density at the offshore location is 1.5 times greater than the power density at the mid-shelf location at the 30 m water depth. At the 50 m water depth, the mean power density is 813.6 and 2,440 W/m^2 at the mid-shelf and offshore locations, respectively. This results in the power density at the offshore location being three times larger than that of the mid-shelf deployment at the 50 m water depth. When comparing these values with

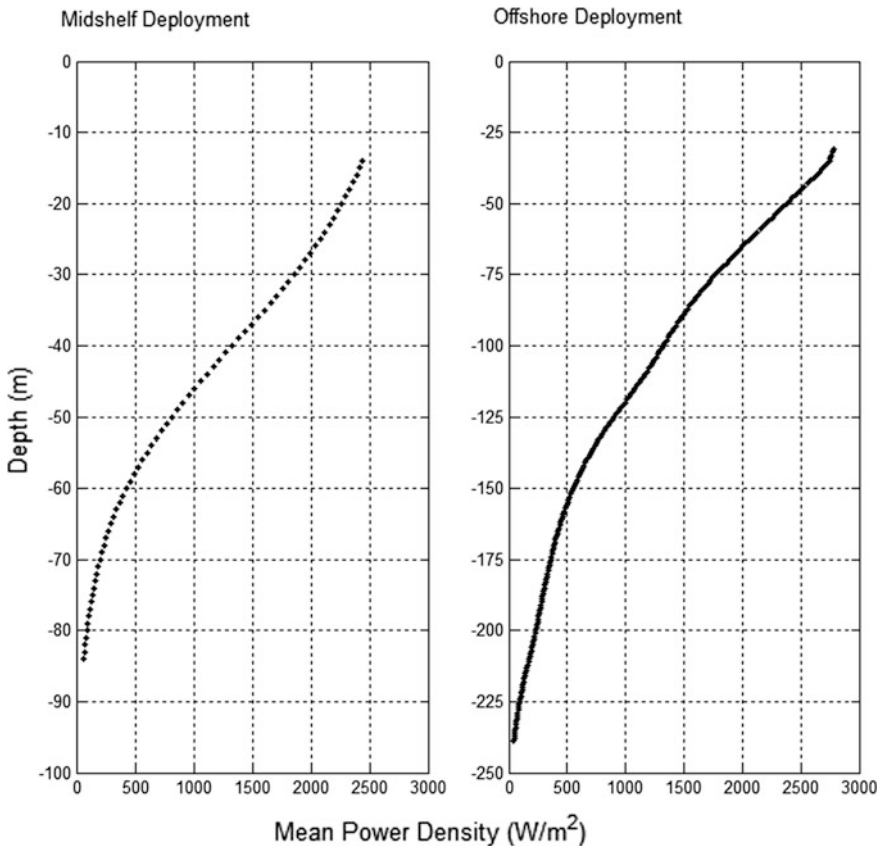

Fig. 12 Mean power density (W/m^2) (Meyer and Van Niekerk 2016)

the current velocity magnitude at the same depths, the cubed relationship between power and velocity magnitude is highlighted.

Directional Analysis

The current direction at each location is described using directional roses plotted at depths of 80, 50, and 30 m in Fig. 13. When the mid-shelf and offshore locations are compared a slight shift in the predominant current direction is seen as the current approaches the shore.

At the offshore location, the predominant current direction is approximately 195° from North where at the mid-shelf location, the predominant current direction is 210° from North. This directionality shows that the current flows in a general south-westerly direction with onshore components.

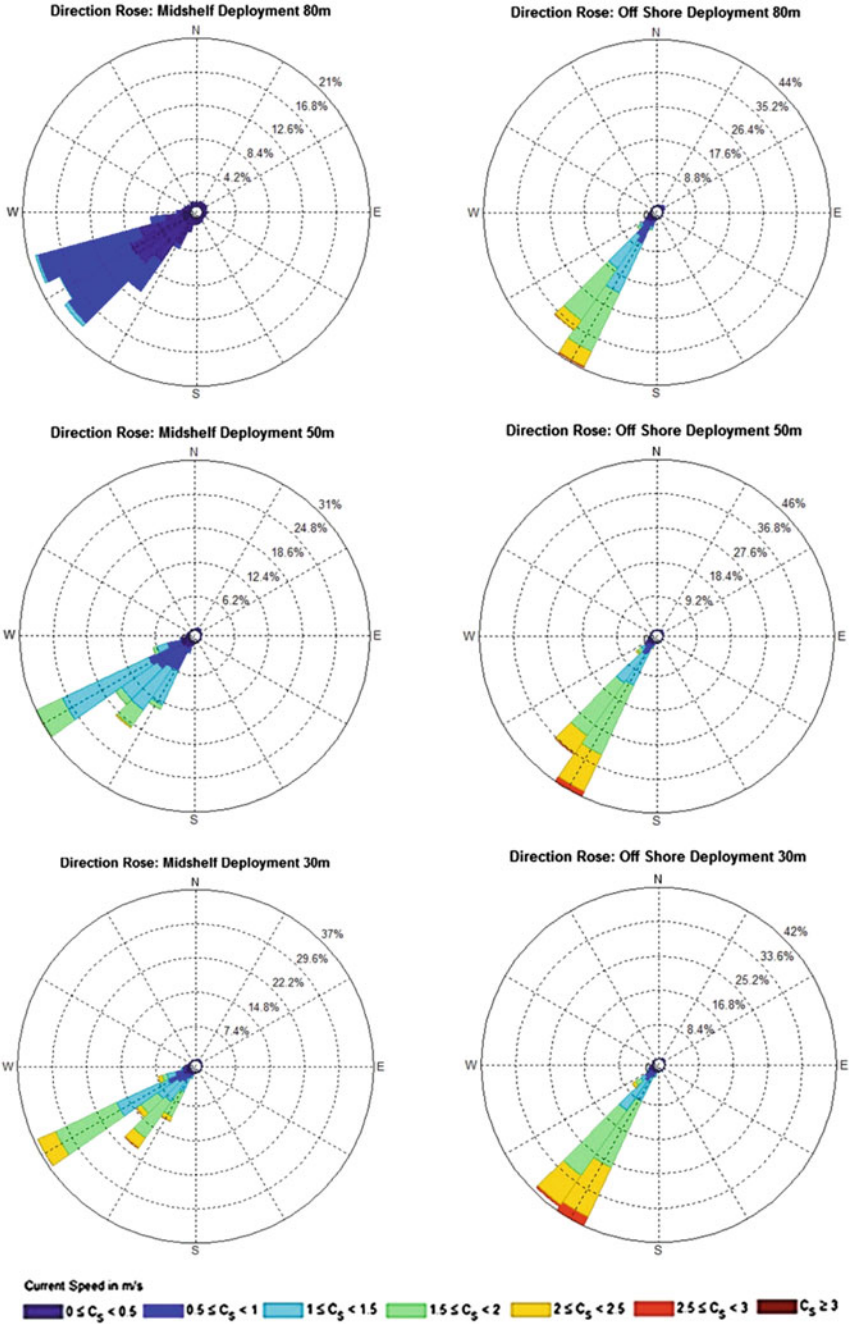

Fig. 13 Mid-shelf location (*left*) and offshore location (*right*): current directional roses at the 80 m (*top*), 50 m (*centre*), and 30 m (*bottom*) water depths (Meyer and Van Niekerk 2016)

At the mid-shelf location, at the 80 m water depth, onshore directional tendencies are seen, whereas at the 50 and 30 m water depths, the directionality ranges between 195° and 210° from North. The current directionality is more constant at the offshore location where only two predominant directions are seen, namely 195° and 200° from North, compared to the mid-shelf deployment that possesses five distinct directional components. This indicates the presence of the core at the offshore location, where the more swift flowing waters reduce the variability in the direction of the current.

The directional roses do not show directionality when the velocity magnitude is zero, but the near-zero velocity magnitude components can be seen to ring the centre of the rose, indicating that during eddies or Natal Pulses the directionality of the current is no longer in the south-westerly direction and current reversals take place.

Figure 14 illustrates the relationship of the standard deviation of direction and the percentage of current reversals with depth below the sea surface. The standard

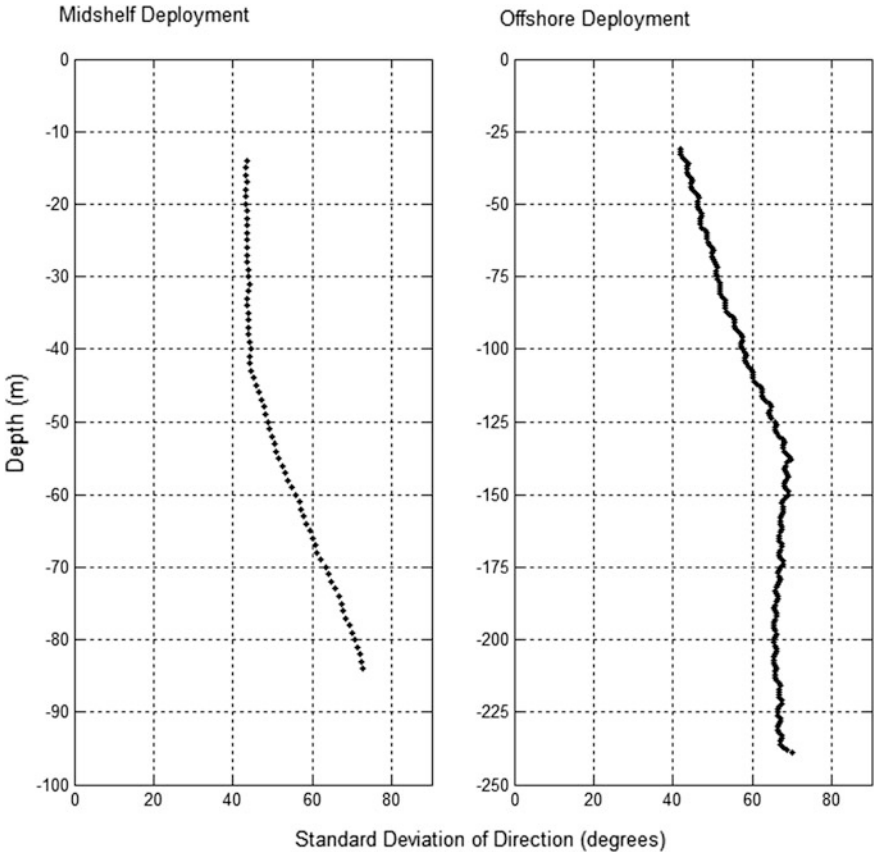

Fig. 14 Standard deviation of flow direction in degrees (Meyer and Van Niekerk 2016)

deviation of the current's direction increases with depth in the upper water column as seen in both mid-shelf and offshore locations. In the offshore location, the variability stabilises below a depth of 137 m. At the 30 m depth, the standard deviation is 43.98° and 40.08° for the mid-shelf and offshore locations, respectively. At a depth of 50 m, the standard deviation is 48.66° and 44.85° for the mid-shelf and offshore locations, respectively. This variability shows that the chosen turbine must be able to adapt to the change in flow direction in order to achieve a maximum power output.

Technical and Environmental Considerations

Technology Considerations

The magnitude of practically extractable power depends on the technology used to harness the current's energy and the power density at which this technology can be deployed. The ocean energy industry as a whole is still immature; ocean current energy technology readiness levels range between TRL 1 and TRL 5 (Mofor et al. 2014). At the time of this study, no ocean current turbines are operating at a commercial scale for energy extraction.

From the results of the current magnitude and directional analysis, it is established that the required technology needs to operate in a flow range of 0.6 and 2 m/s with the mean velocity magnitude occurring between 1 and 1.5 m/s. Further, this technology must be adaptable to change in current direction and must be able to survive the presence of a Natal Pulse that results in a period of zero velocity magnitude.

Of the technology developers developing turbines for tidal applications, Minesto, has expressed interest in adapting the Deep Green 500 kW turbine for ocean current applications with a specific focus on the Gulf Stream (reNews 2014). The Minesto technology holds promise with a design that accelerates the flow velocity through the use of relative motion as the turbine flies through the water in a figure eight pattern. The Minesto Deep Green 500 kW turbine is a tethered turbine with a rated operating speed of 1.6 m/s, cut-in speed of 0.5, and cut-out speed of 2.5 m/s (Minesto 2015). These parameters indicate the suitability of the Minesto Deep Green turbine for deployment in the Agulhas Current.

Another tethered turbine, the Aquantis 2.5 MW C-Plane, has been specially designed to operate in ocean currents (specifically the Gulf Stream) and has a rated speed of 1.6 m/s, which indicates the potential suitability of this device for deployment in ocean current applications (Ecomerit Technologies 2012). However, at the time of this study, no sea trials have been carried out on the C-Plane, so the success of the device is still to be verified. Similarly, IHI Corporation and Toshiba are currently developing a tethered turbine for deployment in the Kuroshio Current.

This device is still in the simulation phase and construction is yet to begin (IHI Corporation 2015).

To compare the variability of the Agulhas Current to other renewable energy resources, a suitable turbine is selected and a capacity factor is obtained from the practically extractable power. Array configuration and spacing are not considered in this research and the capacity factor of a single turbine is presented. The capacity factor is described by the following expression:

$$C_f = \frac{\sum_{i=1}^{N} Powerproduced}{\sum_{i=1}^{N} Turbineratedpower} \tag{2}$$

where N is the total number of time steps over which the capacity factor is calculated.

The theoretical power produced by the turbine is found by using the published power curve (found in Minesto 2011); a polynomial equation is developed to follow this power curve of the turbine using instantaneous velocity magnitude as the input and instantaneous power as the output. For the Minesto turbine that travels through a range of depths, this calculation method makes use of the instantaneous velocity magnitude at one depth, and thus, with the observed decreasing vertical velocity magnitude profile, this method of calculation has the potential to overestimate the total energy output from the system. Furthermore, as outlined by Haas et al. (2013), a single turbine has little to no effect on the upstream characteristics of the current, but a large number of devices can block the flow and reduce the current velocity, and hence reduce the generated power from each device. Thus, it is noted that this methodology cannot be extrapolated to an array of turbines, but rather can be used as a comparative method to identify an energetic site.

The theoretical capacity factors at the mid-shelf and offshore location for the deployment of one Minesto Deep Green 500 kW turbine is presented in Table 5. Table 6 presents the findings from the 500 kW Deep Green turbine that has a rated speed of 1.6 m/s and an optimal operating range of 1.4–2.2 m/s. Similar to the wind turbine industry, the economics of the availability of power versus the magnitude of the power produced must be weighed against one another to find the best-suited turbine. Table 6 shows the theoretical power output and specific yield from the 500 kW Minesto turbine.

Upon examination of Table 5, the capacity factor for the offshore location is significantly higher than the mid-shelf location; there is only a 6% drop in capacity

Table 5 Found capacity factor for the Minesto 500 kW turbine

Minesto 500 kW deep green rated speed of 1.6 m/s		
Depth (m)	Mid-shelf location (%)	Offshore location (%)
30	62	74
50	37	68

Table 6 Theoretical power output at the 30 m depth

	Minesto 500 kW deep green rated speed of 1.6 m/s	
	Annual yield (MWh/annum) (MWh)	Specific yield (kWh/yr-kW installed) (kWh/kW)
Mid-shelf location	2,708	5,416
Offshore location	3,258	6,515

factor between the 30 and 50 m deployment depths. At the mid-shelf location, a 25% drop in capacity factor is seen between the 30 and 50 m deployment depths. Because the mid-shelf location is situated at the edge of the Agulhas Current, the core does not penetrate as deeply as at the offshore location, which results in a drop in velocity that is amplified by the cubed power velocity relation and the subsequent drop in capacity factor.

When comparing the found capacity factors at both locations to the values of other renewable energy resources, the Agulhas Current fairs well. Desktop analysis by Kritzinger (2015), in collaboration with the South African Department of Energy's Independent Power Producer office, approved for publication in 2014, found that for the South African wind resource, the capacity factor for the under-construction or installed wind farms greater than 80 MW ranges from 30 to 45%. If the turbines are installed at 50 m or shallower depths, the found capacity factors are greater than those generated by wind farms for both analysed turbines. A typical capacity factor found for tidal energy extraction ranges from 20 to 30%, and for wave energy extraction devices, it ranges from 15 to 22% (Boyle 2012). The found capacity factors of the Agulhas Current point to a more constant resource in comparison to other renewable energy resources, which indicates a possible contribution to the base-load supply of electricity.

For the 500 kW turbine, the annual electricity production at the offshore location is 3.26 GWh and at the mid-shelf location it is 2.71 GWh. Although the capacity factor and the specific yield of the offshore site is higher than that of the mid-shelf location, the economics of the longer sea cable and increased mooring challenges must be taken into consideration when deciding on an optimal deployment location.

The closest developed technology to that of ocean current turbines is the technology developed to harness tidal stream energy. The rated operating speed of the stationary (gravity or pile mounted) horizontal axis turbines is greater than 2.5 m/s, so these turbines will perform poorly if deployed in the Agulhas Current. Further, the pile mounting or gravity base will prove problematic due to the mooring depth at energetic ocean current sites. Tethered turbines still require development to be optimally deployed in the Agulhas Current; however, Minesto has gained support from the Welsh government and plans to deploy a 10 MW array by 2019 at Holyhead Deep off the coast of Anglesey (Minesto 2015), which indicates progress towards a commercial industry. The turbines used in the analysis are designed

specifically for tidal applications, so the turbine chosen for the Agulhas Current conditions will need to be optimised to maximise the turbine capacity factor and produced energy.

The practically extractable power depends not only on the selected power take-off technology and resource velocity magnitude and directionality, but also is on a number of other factors, as discussed below.

Geotechnical and Mooring Considerations

With respect to current magnitude and direction, the study results indicate that a strong and constant flow of seawater takes place at deeper locations because the current core lies approximately above the 200 m bathymetry line at 28.831 E and 32.507 S. However, the deeper the sounding depth, the larger will be the concerns surrounding the mooring challenges and the drag forces on the turbine tether in order to moor the turbine hub at 30 m below the surface. A stronger and more advanced mooring system will be required at deeper locations, and the economics of higher power production versus the cost of a more robust mooring system must be considered.

Most experience in such applications is related to the mooring of tidal energy extraction devices and this mooring takes place in water depths of less than 100 m. Because there is no oil drilling activity in the area off the eastern South African coast, practical engineering experience gained from working in the required water depths is lacking. When working in water depths of 100 m or less some of the lessons learned from the tidal industry will be transferable, but when working in a tidal resource there is a period of slack water as the tide changes between ebb and flow. The constant flow of the current may prove to be challenging during the deployment and maintenance of ocean current power plants.

To ensure the successful mooring of turbines within the Agulhas Current, the engineering constraints related the environment need to be well understood. For example, the sedimentary and geotechnical properties of the seabed relative to mooring need to be considered. Limited information is available about these characteristics and properties of the subsurface ocean. Documentation of ocean bed topography along the southeast coast of South Africa occurred in the late 1970s and the information presented here is based on the associated maps and findings.

Figure 15 shows a schematic diagram of the shelf section between the latitudes of 28 and 34 S. The region of focus (Sections B and C in Fig. 15) is the outer-shelf region that is dominated by the current. The Agulhas Current dictates the sedimentary transport in this region. Here, the presence of shifting subaqueous dunes and relict gravels is seen. Dune heights of up to 8 m, lengths of 200 m, and dune field widths of a minimum of 10 km have been recorded. The outer-shelf gravels consist of relict sediments produced during the early Flandrain transgression by reworking of fossil algal reef bioherms (Flemming 1978). There is a distinct change in bed form type between the inner shelf and outer shelf, which consist of relict

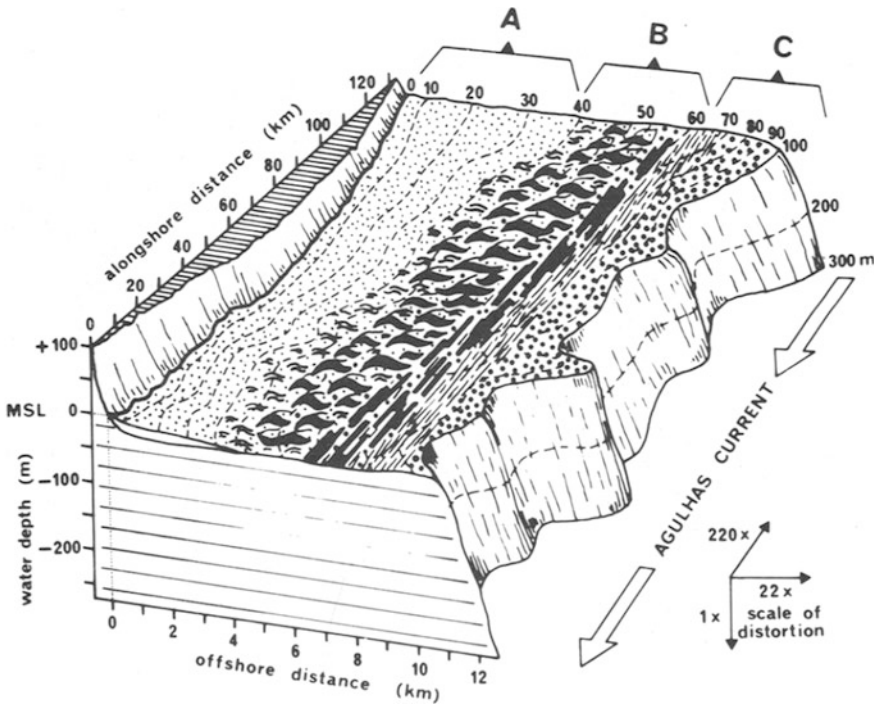

Fig. 15 Schematic block diagram of the shelf section summarising the sedimentary and structural characteristics of the ocean floor topography (Flemming 1980)

carbonate facies. The continental shelf has a very steep slope (~12° gradient) and is dissected by numerous submarine canyons. The outer-shelf region consists of current-generated bed forms such as sand streamers, dunes, and an exposed gravel pavement (Flemming 1980).

The shifting dunes can be problematic because cabling running ashore can be exposed, thereby increasing the risk of scour and requiring more frequent maintenance of the cabling. The presence of the dunes will also increase the amount of dredging that has to be done before bedrock is reached. These dunes are a continuous feature along the southeast margin of the African continent and thus will be encountered continuously along the coast.

An array of turbines will be tethered and anchored to the sea bed. The concerns surrounding this mooring method will be similar to those in other unidirectional currents that have one main loading direction where vortices and vortex shedding may be problematic. The device will have to be robust and designed to withstand geological and environmental extremes while keeping the sophisticated equipment afloat, thus the anchoring foundation must be designed for dynamical loading. The anchors must be designed to resist high cyclic lateral loads and have good scour protection on the tethering cable (Dean 2010).

Another phenomenon within the Agulhas Current is the presence of "Giant Waves" that are unpredictable and have the ability to break large ships in two (Lutjeharms 2006). These waves occur in the core of the current at the landward border, the same position being investigated for device deployment. Although the energy extraction devices will be located at least 20 m below the surface, such extreme conditions must be taken into account when addressing maintenance concerns and the fatigue loading in the device and mooring system.

Very little experience has been gained with respect to mooring considerations in this region, so extensive geotechnical surveys will have to be carried out if ocean current energy becomes a reality.

Commercial Fishing Activities

Figure 16 shows areas of importance to the fisheries industry. The map shows a cost–benefit analysis indicating the zones of high yield. The area of interest for current turbine development lies between East London and Port St John's, and from Fig. 16, it can be seen that this is not a prime area for fishing. This finding is positive because placing a turbine array in this area will help unlock the economic potential of the ocean in this region without interfering with other economic activities or ocean users. This is a preliminary finding; the site-specific effect of the turbine array on commercial and subsistence fish farmers will need to be determined by conducting an environmental impact assessment.

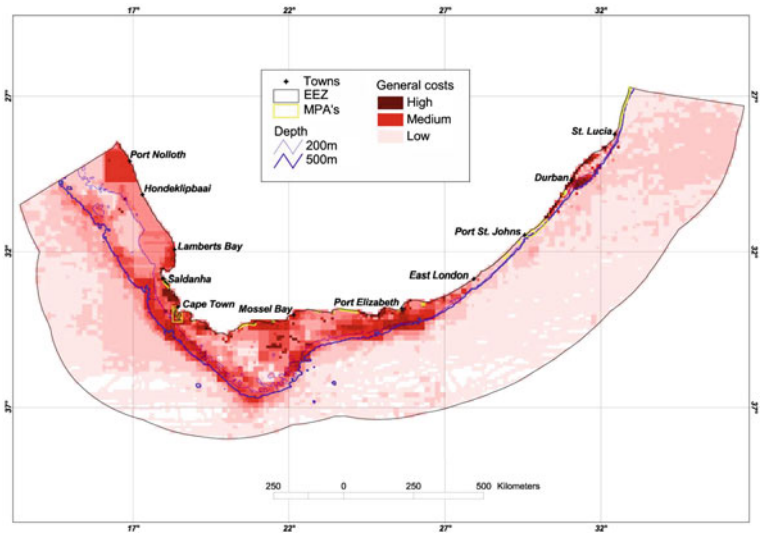

Fig. 16 Map showing the cost benefit to the fisheries industry. The darker areas are of greater importance to the industry in both benthic and pelagic respects (Sink et al. 2011)

Shipping Routes

The shipping route down the east coast of South Africa is an important trade route as illustrated in Fig. 17 by the number of journeys made during a one-year period. The establishment of a turbine array must not hinder this economic activity, and the appropriate depth below the surface must be established. Although the deployment depth of the turbines will take heed of ship wakes, exclusion zones may have to be considered with respect to ship anchoring concerns in the region of turbine deployment.

Existing Infrastructure that Can Consume the Generated Energy

A schematic of the existing Eskom substations is seen in Fig. 18, which indicates the distances from the ADCP deployment locations (mid-shelf and offshore locations indicated by white circles). The mid-shelf site is located 14 km from the shore and 30 km from the nearest medium voltage station. The offshore site is 18 km from shore and 30 km from the nearest medium voltage station. This indicates that there is existing infrastructure to make use of the generated electricity, but an economic analysis must be carried out to determine whether the increased power generated at the offshore location justifies the increase in sea cabling length.

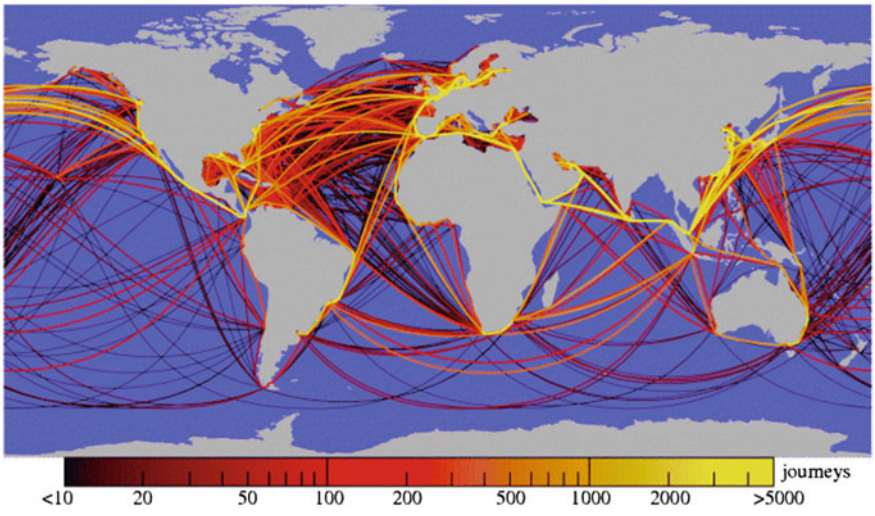

Fig. 17 Trajectories of all cargo ships bigger than 10,000 GT during 2007 (Kaluza et al. 2010)

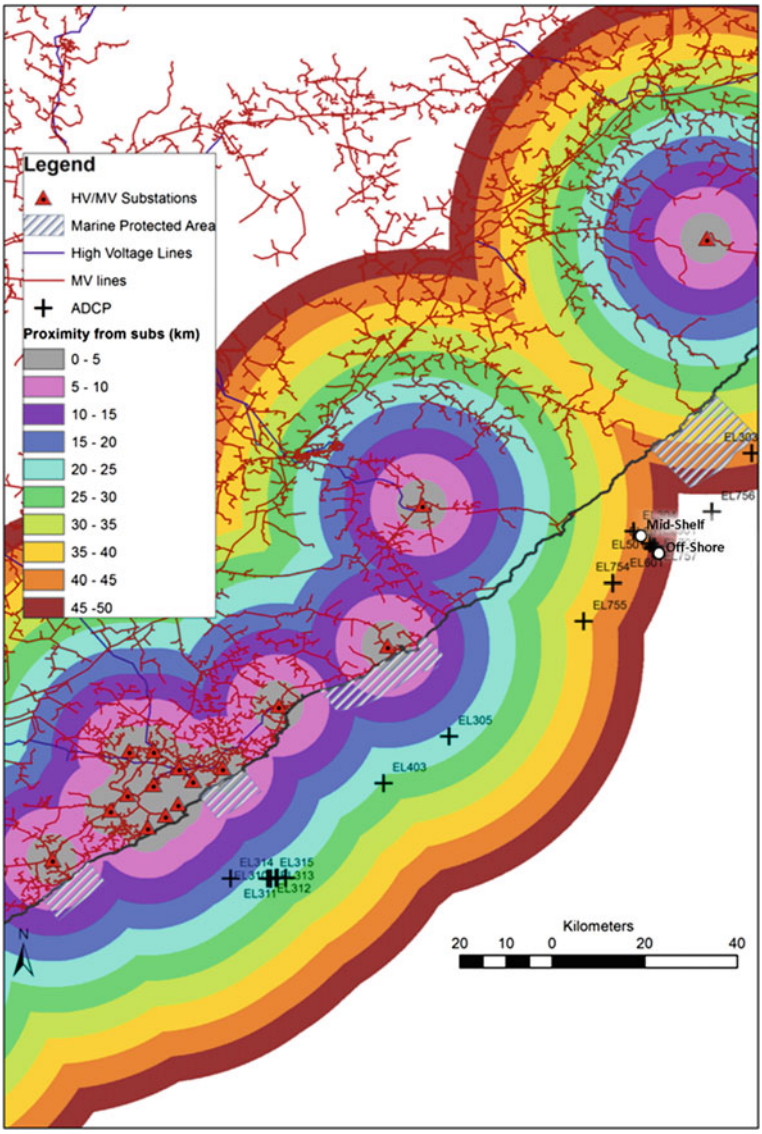

Fig. 18 Position of existing Eskom substations in the region of interest (Meyer et al. 2013)

The distances from the deployment sites to the nearest substation are significantly longer than those seen for tidal sites, but are comparable to offshore wind sites. For offshore wind sites, subsea AC cabling is used for projects located up to approximately 60 km offshore (Norton et al. 2011).

Environmental Impact

The closest existing marine protected area lies 15 km north of the analysed sites. No marine protected areas lie between the selected sites and the closest harbour located on the coast is Port Elizabeth, 350 km southwest of the chosen sites. The positions of the existing and proposed marine protected areas along the South African coastline are seen in Fig. 19. The closest economic hub in this area is East London, which lies south of the analysed sites; thus, no cabling or vessels required for the deployment and maintenance of the devices will pass through marine protected areas. It is also encouraging to notice that the proposed marine protected areas will not cause obstacles in this regard. Furthermore, the chosen turbines are shrouded, which decreases the impact of these devices on marine mammals.

On a larger scale, the environmental impact on the meridional overturning circulation of placing turbines that extract energy from the Agulhas Current has not yet been investigated and the maximum size of a potential power plant is yet to be established. In 2007, the Bureau of Ocean Energy Management published an Environmental Impact Statement (U.S. Department of the Interior Minerals Management Service 2007) in which the effects of deployment of ocean current turbines in the Gulf Stream are considered. The impacts will depend on the technology and array configuration chosen, but typical impacts include reduction in current velocity and energy and possible reduction in wave height in the vicinity of the devices (U.S. Department of the Interior Minerals Management Service 2007). Reduction of wave height will be localised, but the reduction in current energy can affect larger

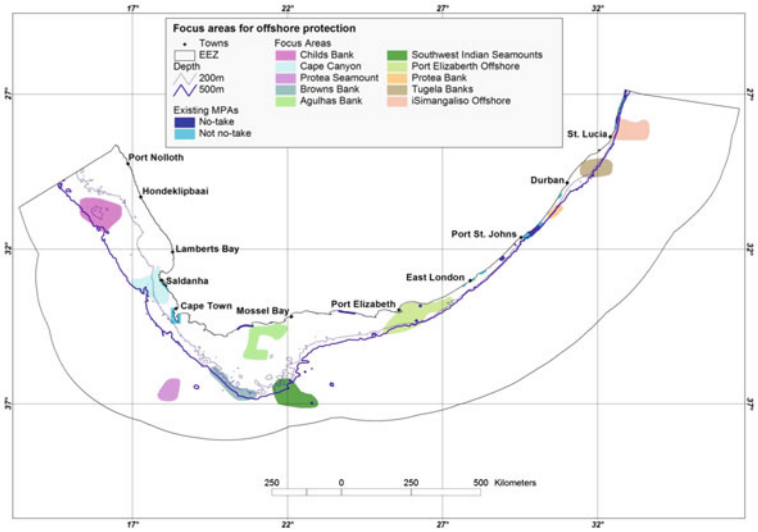

Fig. 19 Existing and proposed marine protected areas around the South African coast (Sink et al. 2011)

systems—namely weather patterns and the interactions of current with nearshore waters.

Using a depth-averaged 2D equation model, Haas et al. (2013) examined the effects of placing an array of turbines in the Gulf Stream. For a limited turbine array, the impact of turbines was found to be primarily confined in the turbine regions with negligible far-field effects. However, as the turbine region increases the region with reduced flow grows accordingly and leads to a reduced flow rate. If the turbine region extends across the core of the Gulf Stream, the energy extraction from the turbines can slow the flow universally across the entire basin. Such impacts within the Agulhas Current will need to be determined through large-scale ocean modelling. The impacts of ocean current turbine systems can be limited by restricting the quantity of energy extracted from the current and maximising the efficiency of the systems deployed. If such mitigations are put in place, this environmental challenge should not result in the discontinuation of ocean current projects.

Regulatory Environment

South Africa has a well-established National Environmental Management: Integrated Coastal Management Act (2008) (ICMA) that regulates the activities along its coastline. Prior to any construction on the coastline, an environmental impact assessment will need to be carried out in accordance with this Act. However, there is a lack of Marine Spatial Planning (MSP) within the Exclusive Economic Zones of South Africa to regulate marine usage by the various stakeholders in the marine environment. The launch of Operation Phakisa has seen the establishment of a formal MSP process for South Africa. The MSP focus areas are aquaculture, mining, shipping, fisheries, and conservation (Marine Protection Services and Governance 2014). Renewable energy has been excluded from this plan, and this can result in uncertainty surrounding the consenting process for marine renewable energy projects.

Other formal permits that will need to be considered in order to obtain consent for a marine renewable energy project include those associated with the National Environmental Management Biodiversity Act, Sea Birds and Seals Protection Act, and National Energy Regulator of South Africa Electricity Regulation Act. This is not necessarily a comprehensive list because each project's permitting will need to be approached on a site-by-site basis.

From the preliminary analysis of other contributing factors, no one factor will cause such a project to be a no-go. The economics of such an endeavour are still a challenge and the environmental concerns will need to be addressed so that renewable energy stakeholders become well-established and welcomed users of the marine environment.

Conclusion About the Best Site

Through the analysis of ADCP, GlobCurrent, and HYCOM data sets along the eastern South African coastline, an area of swift, stable flow in the Agulhas Current has been identified. This area is approximately 100 km northeast of East London, the closet economic hub. One mid-shelf and one offshore site in this area were analysed, and the offshore site was found to be more energetic with higher velocities and reduced directional variability. The mean velocity found at the 30 m depth at the offshore location is 1.59 m/s, and the mean velocity at the mid-shelf location is 1.34 m/s. Ideally, a turbine will operate at a rated speed within this velocity magnitude range.

Unique challenges for exploiting this resource for energy generation exist, including the irregular occurrence of large Agulhas Current meanders (known as Natal Pulses). The comparison between GlobCurrent and HYCOM data and in situ ADCP data was used to determine if this variability can be captured remotely. PCA showed that the GlobCurrent product shows a weaker Agulhas Current with less variability than indicated by the in situ data, and the HYCOM product shows more accurate Agulhas Current velocities but very little variability in the current. Comparison of the ADCP, GlobCurrent, and HYCOM data spectra indicates that the satellite-derived product is able to capture the correct levels of variability in terms of the inverse energy cascade of processes in the ocean, while the modelled data show some limitations in this regard. However, upon closer examination, it is evident that both GlobCurrent and HYCOM data sets only adequately represent scales of variability at the monthly time scale. This latter fact places a significant limiting factor on using these data for prediction to inform stakeholders and highlights the need for further development and improvement of these products.

Nevertheless, in the absence of a spatial and temporally coherent ocean observation system for the Agulhas Current, these data provide useful insights into the modes of variability in the Agulhas Current and their implications for energy production. With the aid of satellite measurements, the presence of Natal Pulses have been found to be predicted approximately 15 days prior to their occurrence at the identified energetic site if tacked from a location higher up the coast. It should be noted, however, that the reduced correlation between in situ and satellite data at the weekly to 10-day time scale may decrease the accuracy of such predications. This prediction will help in minimising the effects of this phenomenon because such periods of no production can be used for scheduled maintenance, and grid planners will have warning enough to mobilise other forms of power generation.

To reduce the barrier of entry into the ocean energy market in South Africa, the challenges facing remote-sensing and assimilative modelling data need to be addressed. There is a critical need for the predictive ocean modelling and satellite remote-sensing community to develop the capabilities to resolve the high spatial–temporal resolution processes needed for accurate characterisation of ocean current energy potential. The new Sentinel series satellites recently launched by the European Space Agency may provide the high-resolution data satellite required.

Regional modelling and data assimilation efforts such as those detailed by Backeberg et al. (2014) are critical for achieving improved predictive skill in the Agulhas Current in particular. The open access nature of these data sets is instrumental in opening the market to future developers as well as in reducing future monitoring and operational costs. If the region of interest is accurately mapped at a high resolution, this knowledge can be used to inform MSP policies so that marine energy extraction activities can be taken into consideration and further advance the industry.

Although a number of engineering and financial issues challenge deployment of a turbine array in the Agulhas Current, if the resource is paired with the correct turbine, the estimated capacity factors compare well with other renewable energy resources; thus, this current holds potential to make a significant contribution to the South African electricity grid.

Acknowledgements The authors would like to acknowledge the South African national utility Eskom for making available the data, without which this research would not have been possible. Dr Backeberg acknowledges joint support from the Nansen-Tutu Centre for Marine Environmental Research, Cape Town, South Africa; the Nansen Environmental and Remote Sensing Center, Bergen, Norway; and the South African National Research Foundation through the Grants 87698 and 91426. This work has also received a grant for computer time from the Norwegian Program for supercomputing (NOTUR project number nn2993 k). Special thanks to Dr Julie Deshayes for her input and guidance in analyzing the spectra. Both the GlobCurrent and HYCOM data used in this study are freely available online at http://www.globcurrent.org and hycom.org, respectively. GlobCurrent products are available for free thanks to European Space Agency funding under GlobCurrent DUE project A0/1-7472/13/I-LG.

References

Backeberg, B. C., Counillon, F., Johannessen, J. A., et al. (2014). *Ocean Dynamics, 64,* 1121. doi:10.1007/s10236-014-0717-6.

Beal, L. M., & Bryden, H. L. (1999). The velocity and vorticity structure of the Agulhas Current at 32 S. *Journal of Geophysical Research, 104*(C3), 5151–5176.

Biastoch, A., Lutjeharms, J. R. E., Böning, C. W., & Scheinert, M. (2008b). Mesoscale perturbations control inter-ocean exchange south of Africa. *Geophysical Research Letters*, *35* (L20602).

Boyle, G. (2012). *Renewable energy* (3rd ed.). Oxford: Oxford University Press.

Bryden, H. L., Beal, L. M., & Duncan, L. M. (2005). Structure and transport of the Agulhas Current and its temporal variability. *Journal of Oceanography, 61,* 479–492.

Chang, Y.-C., Chu, P. C., & Tseng, R.-S. (2015). Site selection of ocean current power generation from drifter measurements. *Renewable Energy*, *80*, 737–745. doi:10.1016/j.renene.2015.03.003.

Chen, F. (2010). Kuroshio power plant development plan. *Renewable and Sustainable Energy Reviews*, *14*(9), 2655–2668. doi:10.1016/j.rser.2010.07.070.

Cummings, J. A. (2005). Operational multivariate ocean data assimilation. *Quarterly Journal* of the *Royal Meteorological Society*, *Part C*, *131*, (613), 3583–3604.

Dean, E. (2010). *Offshore geotechnical engineering*. London: Thomas Telford Limited.

Dohan, K., & Maximenko, N. (2010). Monitoring ocean currents with satellite sensors. *Oceanography, 23*(4), 94–103. doi:10.5670/oceanog.2010.08.

Ducet, N., Le Traon, P.-Y., & Reverdin, G. (2000). Global high-resolution mapping of ocean circulation from TOPEX/Poseidon and ERS-1 and -2. *Journal Geophysical Research, 105,* 19477–19498.

Duerr, A. S., & Dhanak, M. R. (2012). An assessment of the hydrokinetic energy resource of the Florida current. *IEEE Journal of Oceanic Engineering, 37*(2), 281–293.

Ecomerit Technologies. (2012). Aquantis [Online]. http://www.ecomerittech.com/aquantis.php. [2015, February 7].

Ekman, V. W. (1905). On the influence of the Earth's rotation on ocean currents. *Archives of Mathematics, Astronomy, and Physics, 2*(11), 1–52.

Flemming, B. (1978). Underwater Sand Dunes along the Southeast African continental Margin-Observations and implications. *Marine Geology, 26,* 177–198.

Flemming, B. (1980). Sand transport and bedform patterns on the continental shelf between Durban and Port Elizabeth (Southeast African Continental Margin). *Sedimentary Geology, 26,* 179–205.

Fox, D. N., Teague, W. J., Barron, C. N., Carnes, M. R., & Lee, C. M. (2002). The modular ocean data assimilation system (MODAS). *Journal of Atmospheric and Oceanic Technology, 19,* 240–252.

Gründlingh, M. L. (1983). On the course of the Agulhas Current. *South African Geographical Journal, 65,* 49–57.

Haas, K., et al. (2013). Assessment of Energy Production Potential from Ocean Currents along the United States Coastline, Atlanta.

IHI Corporation, Power Generation Using the Kuroshio Current. (n.d.). Retrieved November 26, 2015 from http://www.ihi.co.jp/var/ezwebin_site/storage/original/application/149ee9de3149aba2e1215fd5f9cd46ec.pdf.

Kaluza, P., Kolzsch, A., Gastner, M. T., & Blasius, B. (2010). The complex network of global cargo ship movements. *Journal of the Royal Society, 7,* 1093–1103.

Kritzinger, K. (2015). Personal Communication. 23 February, Stellenbosch.

Krug, M. J., & Tournadre, J. (2012). Satellite observations of an annual cycle in the Agulhas Current. *Geophysical Research Letters, 39,* L15607.

Lutjeharms, J. (2006). *The Agulhas Current*. Berlin: Springer.

Lutjeharms, J. R. E., & Roberts, H. R. (1988). The natal pulse: An extreme transient on the Agulhas Current. *Journal Geophysical Research, 93,* 631–645.

Marine Protection Services and Governance. (2014). *Unlocking the economic potential of South Africa's Oceans*. Durban: Operation Phakisa.

Meehl, G. A., Goddard, L., Murphy, J., Stouffer, R. J., Boer, G., Danabasoglu, G., et al. (2009). Decadal prediction. *Bulletin of the American Meteorological Society*, *90*, 14671485.

Meyer, I., & Van Niekerk, J. L. (2016). International Journal of Marine Energy Towards a practical resource assessment of the extractable energy in the Agulhas ocean current. *International Journal of Marine Energy*, *16*, 116–132. doi:10.1016/j.ijome.2016.05.010.

Meyer, I., Reinecke, J., Roberts, M., & van Niekerk, J. L. (2013). *Assessment of the ocean energy resources off the South African coast*. Stellenbosch: Centre for Renewable and Sustainable Energy Studies, Stellenbosch University.

Meyer, I., Reinecke, J., & Van Niekerk, J. L. (2014). Resource assessment of the Agulhas Current for the purpose of marine energy extraction. In *5th International conference on ocean energy*. Halifax.

Minesto. (2011). DG-12 *Technical Specifications*. Sweden: Minesto.

Minesto. (2015). Minesto—Power from Tidal and Ocean Currents, (n.d.). Retrieved November 23, 2015 from http://minesto.com/.

Mofor, L., Goldsmith, J., & Jones, F. (2014). Ocean *energy: technology readiness, patents, development status and outlook*. Bonn: International Renewable Energy Agency [Online]. http://www.irena.org/DocumentDownloads/Publications/IRENA_Ocean_Energy_report_2014.pdf. [2015, February 10].

Norton, M., Mansoldo, A., & Rivera, A. (2011). Offshore *grid study: analysis of the appropriate architecture of an irish offshore network*. Dublin: EirGrid Plc [Online]. http://www.eirgrid.com/media/2257_Offshore_Grid_Study_FA.pdf. [2015, June 20].

Renewable Energy Caribbean. (2014). Ocean Current Energy, an Untapped Resource. https://renewableenergycaribbean.com/2014/09/01/the-potential-of-ocean-current-energy/.

reNews. (2014). Minesto heading for Florida. http://renews.biz/68909/minesto-heading-for-florida/.

Rio, M.-H., Mulet, S., & Picot, N. (2014). Beyond GOCE for the ocean circulation estimate: Synergetic use of altimetry, gravimetry, and in situ data provides new insight into geostrophic and Ekman currents. *Geophysical Research Letters*, *41*. doi:10.1002/2014GL061773.

Robinson, I. S. (2004). *Measuring the oceans from space*. Berlin: Springer.

Rouault, M. J., & Penven, P. (2011). New perspectives on the natal pulse from satellite observations. *Journal of Geophysical Research, 116,* C07013.

Rouault, M. J., Mouche, A., Collard, F., Johannessen, J. A., & Chapron, B. (2010). Mapping the Agulhas Current from space: An assessment of ASAR surface current velocities. *Journal of Geophysical Research, 115,* C10026.

Scott, R. B., & Wang, F. (2005). Direct evidence of an oceanic inverse kinetic energy cascade from satellite altimetry. *Journal of Physical Oceanography, 35,* 1650–1666.

Sink, K. Sink, K. J., Attwood, C. G., Lombard, A. T., Grantham, H., Leslie, R., et al. (2011). *Spatial planning to identify focus areas for offshore biodiversity protection in South Africa: Final report for the offshore marine protected area project*. Cape Town: South African National Biodiversity Institute.

U.S. Department of the Interior Minerals Management Service. (2007). *Programmatic environmental impact statement for alternative energy development and production and alternate use of facilities on the outer continental shelf: Final environmental impact statement*. USA: Bureau of Ocean Energy Management.

Van Zwieten, J. H., et al. (2014). Evaluation of HYCOM as a tool for ocean current energy assessment.

Van zwieten, J. H., et al. (2015). SS marine renewable Energy—Ocean current turbine mooring. In *Offshore technology conference*. Houston.

Wold, S., Esbensen, K., & Geladi, P. (1987). Principal component analysis. *Chemometrics and Intelligent Laboratory Systems, 2,* 37–52.